applied sciences

MDPI

Article

Denudation Recovery and Prototype Basin Structural Pattern During the Faulting Period in the Southern Part of the Central Depression Area of the Songliao Basin

Jiachang Zhang [1], Tao Li [1,*], Jia Hu [2], Hui Wang [3], Tong Yue [1], Jiayu Liu [1] and Yuxun Cai [1]

[1] School of Earth Sciences, Yangtze University, Wuhan 430100, China; 15981401722@163.com (J.Z.); 13343469175@163.com (T.Y.); 18761013123@163.com (J.L.); caiyuxun0605@163.com (Y.C.)
[2] Institute of Geophysical Exploration, PetroChina Jilin Oilfield Company, Jilin 138000, China; 15195525718@163.com
[3] Exploration and Development Research Institute of Daqing Oilfield Co., Ltd., Daqing 163712, China; 15926425213@163.com
* Correspondence: litaoyangtze@163.com

Abstract: The Changling Depression, located in the southern part of the central depression zone of the Songliao Basin, is characterized by complex structures and has been shaped by multiple phases of tectonic activity. The strata in this region have undergone significant uplift and denudation, resulting in an incomplete understanding of the prototype basin and hindering progress in oil and gas exploration. To better understand the geological characteristics and exploration potential of the Changling Depression, this study begins with the reconstruction of denudation amounts. Using the stratigraphic trend extrapolation method, the denudation of strata during the faulting period of the Changling Depression is quantified. By combining the denudation thickness with the remaining strata thickness, the original strata thickness is restored. Employing MOVE 2018version and Petrel 2021version software, the paleogeomorphology of different geological periods is reconstructed. Through an analysis of the prototype basin's structure, its evolution history, sedimentary filling patterns, and paleogeomorphological features, it is determined that the maximum depositional thickness and rate during the Huoshiling period occurred in the Shenzijing, Heidimiao, and Fulongquan areas, with strong central deposition that weakened toward the north and south. During the Shahezi period, depositional thickness and rates exhibited a pattern of weaker deposition in the south and stronger in the north. In the Yingcheng Formation–Denglouku Formation period, the basin entered a subsidence phase, with an expanded range of strata subsidence. During the Denglouku period, the Qianbei area experienced strong deposition, while the Heidimiao area saw even more pronounced deposition; in contrast, the Shenzijing area displayed very weak depositional activity. The study reveals a south-to-north migration of lateral subsidence centers over time, influenced by left-lateral tectonic forces, reflecting a shift in the dominant influence pattern. These findings clarify the morphology of the prototype basin and the distribution and migration of subsidence centers across different periods, providing valuable insights that will facilitate deeper oil and gas exploration efforts in the Changling Depression.

Keywords: changling depression; denudation restoration; prototype basin restoration; paleogeomorphic restoration; sedimentary center

check for updates

Academic Editor: Nikolaos Koukouzas

Received: 13 January 2025
Revised: 8 March 2025
Accepted: 12 March 2025
Published: 13 March 2025

Citation: Zhang, J.; Li, T.; Hu, J.; Wang, H.; Yue, T.; Liu, J.; Cai, Y. Denudation Recovery and Prototype Basin Structural Pattern During the Faulting Period in the Southern Part of the Central Depression Area of the Songliao Basin. *Appl. Sci.* **2025**, *15*, 3149. https://doi.org/10.3390/app15063149

Copyright: © 2025 by the authors. Licensee MDPI, Basel, Switzerland. This article is an open access article distributed under the terms and conditions of the Creative Commons Attribution (CC BY) license (https://creativecommons.org/licenses/by/4.0/).

1. Introduction

The Songliao Basin, located in northeastern China, is a continental basin formed during the Mesozoic–Cenozoic era, rich in oil and gas resources. The Changling Graben, the largest fault depression group in the southern part of the Songliao Basin, features a typical double-layer structure of fault depression superposition [1,2]. Significant breakthroughs were made with the deployment of the Changshen 40 and 41 wells in the Changling Graben, revealing the vast resource potential of deep tight gas [3–5]. Since the Early Cretaceous Huoshiling period, the Changling Graben has undergone multiple phases of complex tectonic movements, greatly altering the basin's landscape. According to the "prototype controls source" theory, the development of source rocks is influenced by the basin prototype during their formation period, such as basin type, paleogeomorphological features, and paleo-depositional environments [6]. To further analyze the deep oil and gas exploration potential of the Changling Graben, it is necessary to restore the basin prototype, clarify the tectonic movements the basin has experienced, and define the impact of later tectonic movements on the basin [6–10]. The uplift and denudation of strata can alter the burial history of the basin, affecting the generation, migration, and preservation conditions of oil and gas [11–15]. Therefore, reconstructing paleogeomorphology combined with denudation amounts can restore the sedimentary records affected by denudation and depict the basin's appearance during the deposition period. Analyzing the prototype basin by integrating basin structure and its evolution, sedimentary fill characteristics, and paleogeomorphological features can summarize the basin's evolutionary laws, providing important evidence for the tectonic evolution of the Songliao Basin [16–18].

Previous studies on the protolithic basin of the Changling Graben have primarily focused on individual graben layers, lacking a systematic restoration of regional denudation amounts across the entire graben [19,20]. Currently, the study area has achieved full coverage of 3D seismic data, with partial completion of secondary acquisition. Various methods exist for calculating stratigraphic denudation amounts, such as the stratigraphic structural trend extrapolation method, the acoustic well logging method, and the wave equation analysis method. In this study, the collected data include acoustic well logging data and seismic data. However, since the upper part of the strata in the Changling Graben period experienced much greater subsidence than denudation, the well logging data do not conform to the principles of sedimentation and compaction, making it impossible to calculate the denudation amount of the graben period strata using well data [21–27]. Consequently, the stratigraphic structural trend extrapolation method was selected to restore the denudation volume of the graben period strata from point to line to surface [28]. Based on the denudation volume and the residual strata, the original depositional thickness of the strata was reconstructed. By integrating the basin structure and evolution, sedimentary filling characteristics, and paleotopography, the protolithic basin of different periods was analyzed, and the patterns of subsidence filling and tectonic evolution were summarized. This analysis provides valuable support for the selection of favorable exploration zones.

2. Geological Background

The Changling Graben is located in the southern part of the Central Depression Zone of the Songliao Basin, extending in a northeasterly direction [29–31]. Controlled by the basement master faults formed during the Late Jurassic to Early Cretaceous period, multiple secondary grabens were formed, such as the Da'an Graben, Qibei Trough, Gudianzi Graben, Shenzijing Trough, Hashitu Trough, Chaganhua Trough, Fulongquan Trough, Heidimiao Trough, and Longfengshan Trough, etc. (Figure 1). Above the Cretaceous basement, the graben period strata mainly include the Huoshiling Formation, Shahezi Formation,

Yingcheng Formation, and the Denglouku Formation during the fault subsided transition period (Figure 2).

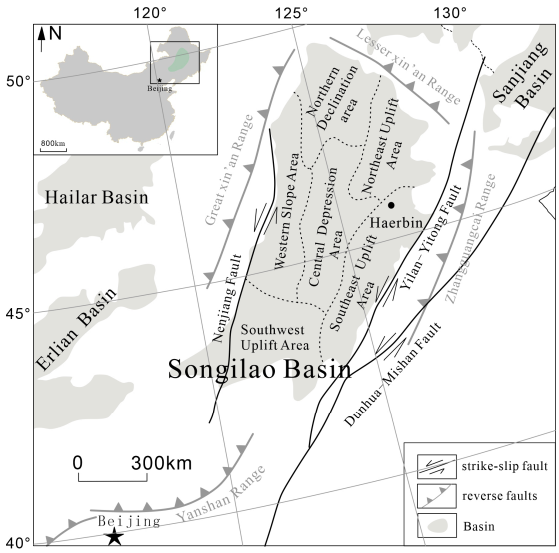


Figure 1. Location map of the Songliao Basin.

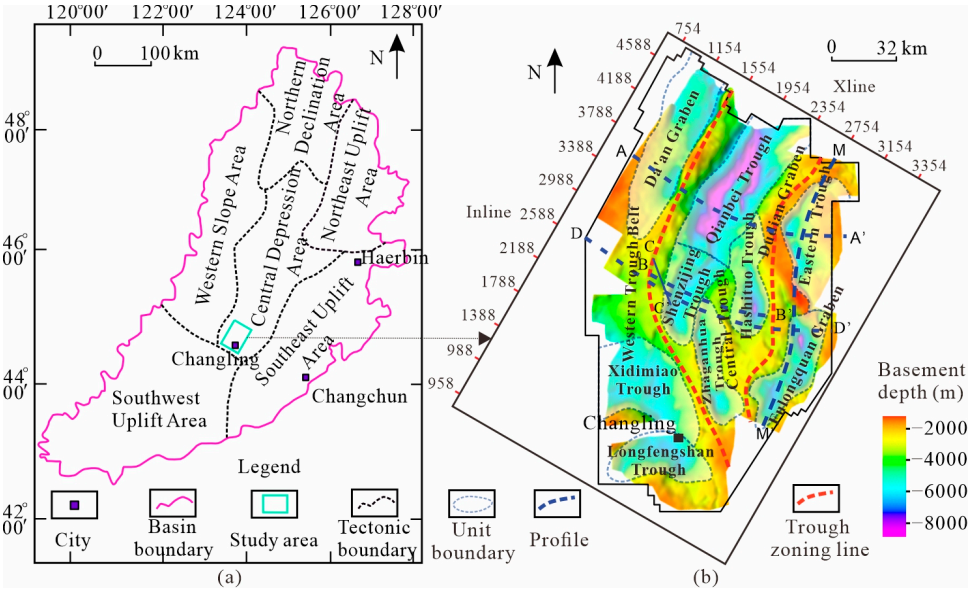


Figure 2. Geological location of the Changling Graben (**a**) and the division of the secondary troughs within the Changling Graben (**b**).

During the deposition period of the Huoshiling Formation, influenced by the rapid oblique subduction of the Izanagi Plate in a NNW direction toward the Eurasian continent, the Changling Graben was subjected to a sinistral transpressive tectonic stress field. This led to the development of a series of NNE-trending sinistral transpressive faults and relatively smaller-scale NW-trending extensional faults within the basin [32,33]. Under the control of these faults, multiple graben and half-graben secondary depressions formed, laying the foundation for the later development of fault depressions and preliminarily establishing the basic structural framework of the fault depression basin. The overall pattern was characterized by a wider and deeper northern part and a narrower and shallower southern part. Building on the previously eroded and leveled Jurassic strata, the basin entered the fault depression stage, with strata widely distributed and relatively thick within the basin. By the end of the Huoshiling Formation deposition period, significant

volcanic activity caused topographic variations, leading to localized denudation of the Huoshiling Formation and the formation of the T_4^2 unconformity surface [34–36]. The Shahezi Formation deposition period marked the intense fault depression stage of the basin. The activity of the fault-controlled depressions was strong, governing the sedimentation and filling of the depressions and promoting the development and expansion of secondary sags. The basin continued to extend and subside [37,38]. By the end of the Shahezi Formation deposition period, localized areas experienced some degree of compressional inversion, resulting in the denudation of the top strata and the formation of the T_4^1 unconformity surface [39–41]. During the Yingcheng Formation deposition period, the basin entered the waning stage of fault depression. The sedimentary characteristics of the strata were mainly characterized by infilling and leveling, accompanied by volcanic eruptions, which caused localized structural inversion and the formation of the T_4 unconformity surface [42,43]. In the deposition period of the Denglouku Formation, the fault-controlled depressions continued to be active in the early stage, with non-uniform crustal subsidence. During this stage, the scale of the faults decreased, primarily manifested as a reduction in fault displacement. This resulted in the lower Denglouku strata being significantly controlled by faults, exhibiting fault depression characteristics [44–46]. However, the subsidence range of the Denglouku Formation was notably larger than that of the lower fault depression layers, also displaying characteristics of a depression. By the end of this period, a brief tectonic inversion occurred, forming the T_3 unconformity surface(Figure 3). From this point onward, the Changling Graben entered the depression stage, exhibiting a typical fault depression superimposed structure in cross-section. The east–west direction displayed a half-graben–horst-graben–horst-half-graben pattern, characterized by a zonal distribution of three grabens and two horsts(Figure 4) [47–49].

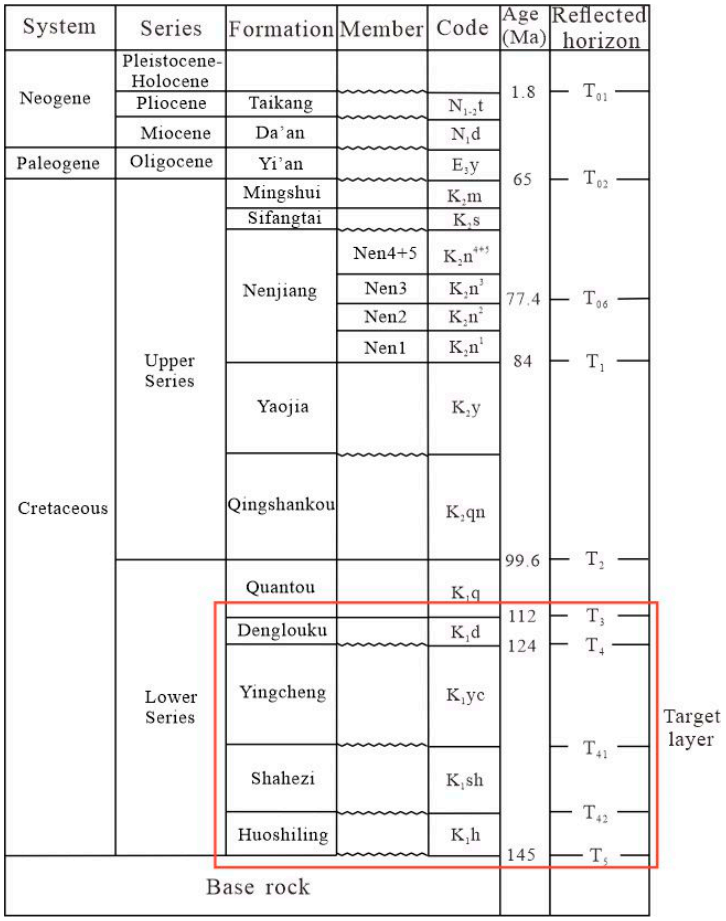


Figure 3. Stratigraphic units in the study area.

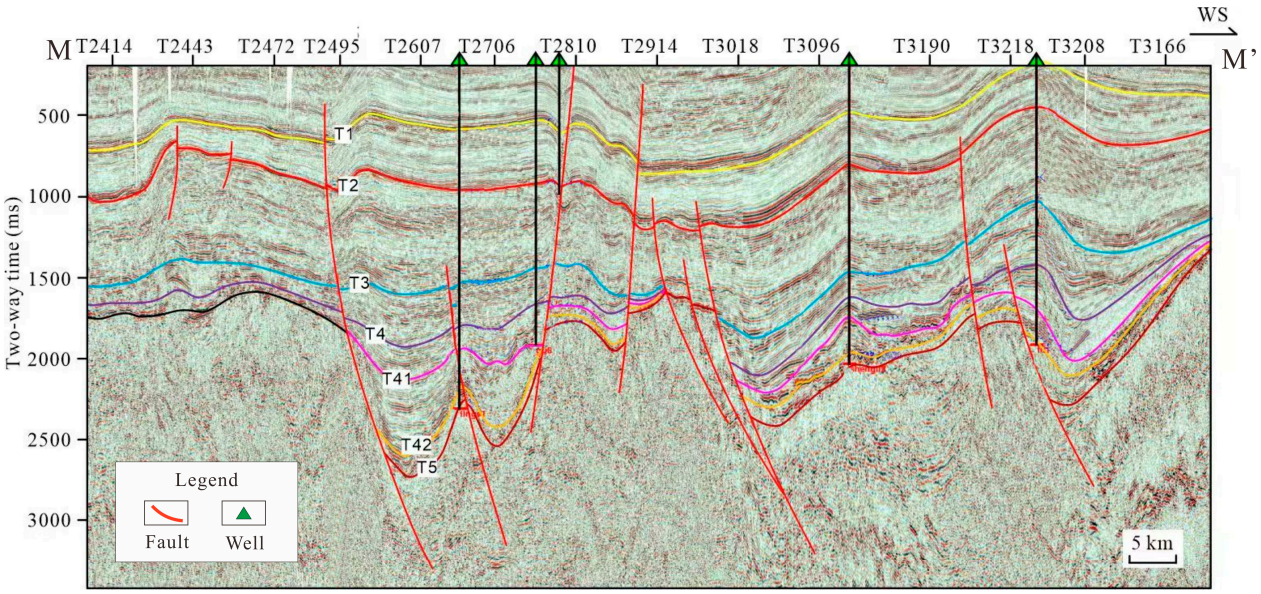


Figure 4. Typical geological cross-section of Changling Graben (section location in (M,M')).

3. Databases and Methods

3.1. Seismic Data

Currently, extensive seismic exploration has been conducted in the Changling Graben of the Songliao Basin, providing valuable data for studying deep structures and strata (Figure 5). This study utilizes the latest 3D seismic data (40 m × 40 m) provided by PetroChina, along with geological and well-log data. The 3D seismic data covers an area of approximately 13,000 km^2, achieving full 3D coverage with good seismic imaging quality and clear seismic reflection structural features. This ensures reliable support for systematically analyzing the structural and sedimentary filling characteristics of the Changling Graben's various sags. Based on the 3D seismic data, five representative crosslines and three inlines were selected. Through detailed stratigraphic and fault interpretation of these profiles, the regional geological framework characteristics of the Changling Graben were summarized. By utilizing the residual strata dip and the convergence trends of internal seismic reflectors, combined with the regional geological background of the Songliao Basin, a "point-line-surface" approach was applied to restore the denudation across the entire area. The denudation amounts for the aforementioned four denudation periods in the Changling Graben were restored at a density of 16 × 16, involving a total of 400 seismic profiles. By analyzing the distribution characteristics of denudation amounts and the residual strata distribution patterns, the tectonic framework of the prototype basin was reconstructed. Combined with the tectonic background of the Songliao Basin, the evolutionary characteristics of the Changling Graben were analyzed, and the subsidence features and evolutionary patterns were summarized [50].

Leveraging the orientation of the residual strata obtained from seismic data and the convergence patterns of co-phase axes within these strata, combined with the regional geological context of the Songliao Basin, this study systematically analyzes and estimates the denudation volumes for the four identified periods of denudation within the Changling Graben. By examining the distribution of denudation volumes and the spatial patterns of the remaining strata [51–53], the study reconstructs the original structural framework of the basin. Integrating this with the tectonic setting of the Songliao Basin, the study elucidates the evolutionary characteristics of the Changling Graben through various stages, highlighting the sedimentological features and underlying evolutionary trends.

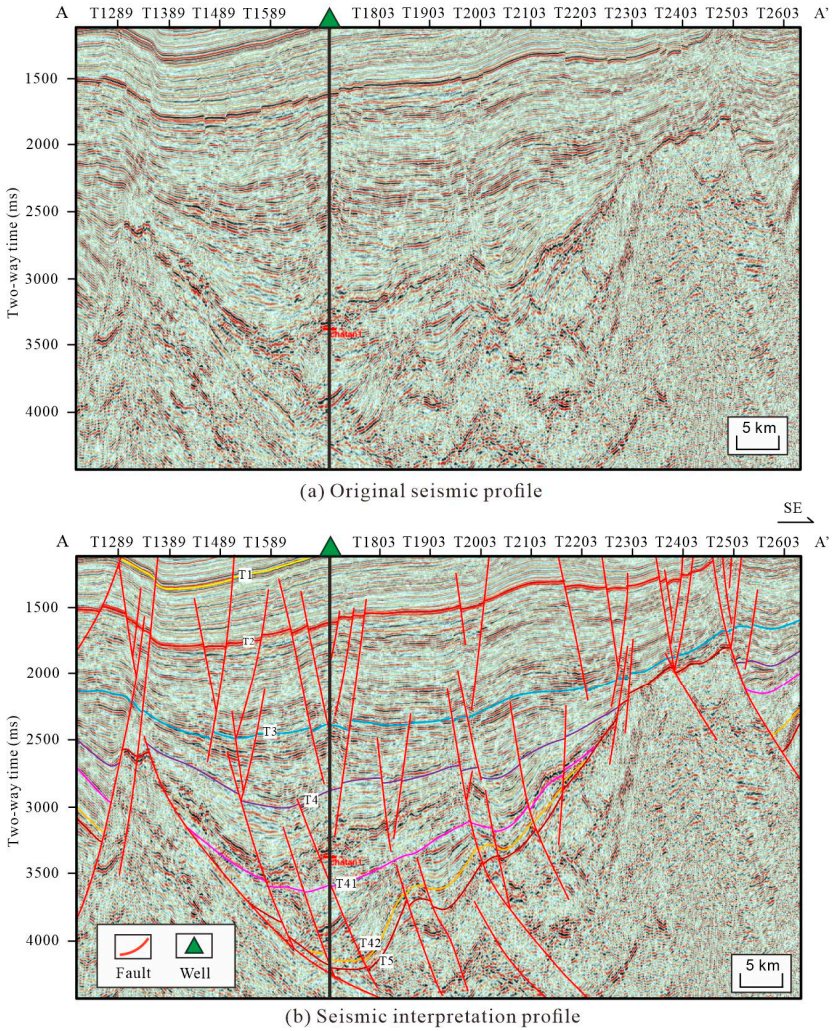


Figure 5. Typical seismic profile of Changling Graben (the profile location is shown in Figure 1). Notes: (**a**) original seismic profile; (**b**) seismic interpretation profile.

3.2. Restoration Method of Formation Denudation

Numerous methods are currently available for calculating stratigraphic denudation, including the stratigraphic structural trend extrapolation method, the acoustic well logging curve method, and the wave equation analysis method [54,55]. Each method possesses distinct advantages and is applicable under specific conditions. The calculation of stratigraphic denudation must be carefully aligned with the tectonic evolution context of the study area to select the most appropriate method for restoring denudation volumes, thereby ensuring the reliability and applicability of the results [56,57]. While most of these methods yield denudation data at discrete points, the stratigraphic structural trend extrapolation method emerges as the most effective approach for achieving a comprehensive understanding of the planar distribution of denudation.

The acoustic wave time difference method is widely employed for calculating denudation volumes. Initially, we assessed the applicability of this method. The method is based on the assumption that there is a consistent exponential relationship between the acoustic wave time difference in rocks and their depth, provided that the compaction pattern of the strata remains unchanged [58,59]. By statistically fitting the acoustic wave time difference and depths of undepleted strata, a standard exponential compaction trend curve is derived. Extrapolating this curve to where the acoustic wave time difference (Δt) equals the initial acoustic wave time difference (Δt_0) delineates the paleosurface; the interval between this

paleosurface and the unconformity represents the denudation thickness (Figure 6). The application of this method is subject to specific criteria. Generally, it is applicable when the pressure exerted by the newer strata above the denudation surface on the underlying residual strata is less than or equal to the pressure exerted by the eroded strata prior to denudation. This ensures the integrity of the compaction curve for the residual mudstones in the lower sections. However, drilling data from the study area reveal that the combined thickness of the graben strata and the overlying newly deposited strata exceeds 500 m, significantly surpassing the thickness of the eroded strata. Additionally, the deposition process was marked by vigorous activity along the controlling fault and the formation of extensive volcanic rocks. Consequently, the logging data do not conform to the expected sedimentation and compaction patterns, making it impossible to generate a reliable compaction curve and, thus, to calculate the denudation thickness. Therefore, the acoustic wave time difference method is not suitable for determining the denudation thickness of the strata in this context.

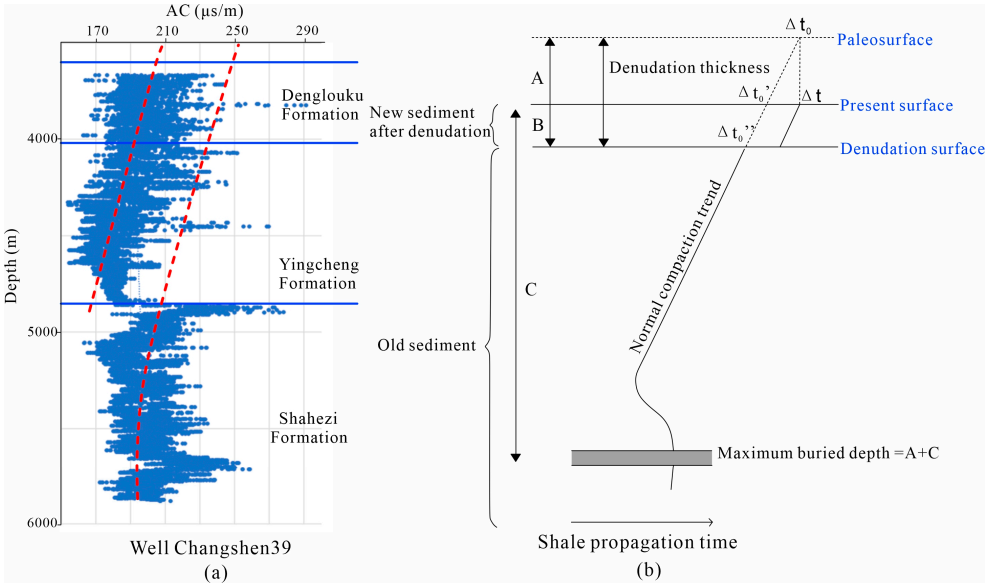


Figure 6. Schematic diagram of denudation recovery using the acoustic wave time difference method. Notes: (**a**) acoustic wave time difference curve of well Changshen 39; (**b**) basic principle of the acoustic wave time difference method.

Denudation can lead to the formation of unconformities between stratigraphic layers, with each unconformity potentially indicating multiple phases of uplift and denudation. By integrating the analysis of tectonic activities and regional geological settings within the study area, the stratigraphic structural trend extrapolation method proves to be highly applicable. This methodology utilizes the orientation of residual strata and the convergence trend of co-phase axes to reconstruct the pre-denudation strike, thereby estimating the magnitude and spatial distribution of denudation during key tectonic episodes. It provides a means of quantifying the multi-episodic denudation volumes of the strata [60,61]. The integration of drilling data and 3D seismic data elucidates distinct unconformities between the Huoshiling Formation, Shahezi Formation, Yingcheng Formation, and Denglouku Formation with the overlying strata in the Changling Graben. Particularly in the Shenzijing–Hashitu region, there is a notable disparity in the strike of the overlying and underlying strata. These unconformities, characterized by truncation and onlap contact relationships on seismic profiles, indicate that the strata underwent tectonic deformation prior to denudation. The study area exhibits two distinct types of denudation (Figure 7), with the strata beneath the unconformities displaying clear truncation features.

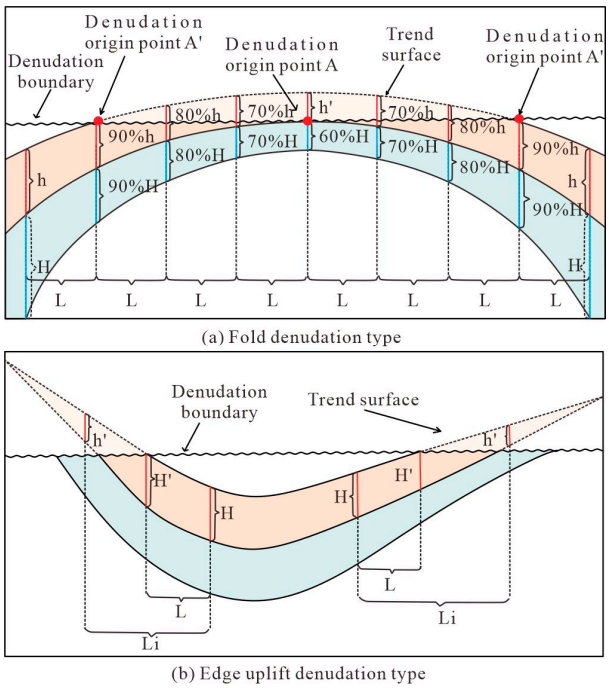


Figure 7. Denudation types of Changling Graben. (**a**) Fold denudation type; (**b**) marginal uplift denudation type. H represents the residual stratigraphic thickness, and h′ represents the denudation thickness.

By carefully analyzing the orientation of the residual strata and the convergence patterns at internal layer interfaces, we can identify areas that have remained unaffected by denudation. By measuring the degree of thinning over equivalent horizontal distances, we can extend our findings to eroded zones, reconstructing the eroded thickness by adhering to the principle of a uniform rate of thinning. This method allows us to estimate the extent of denudation in the affected areas, as illustrated in Figure 8.

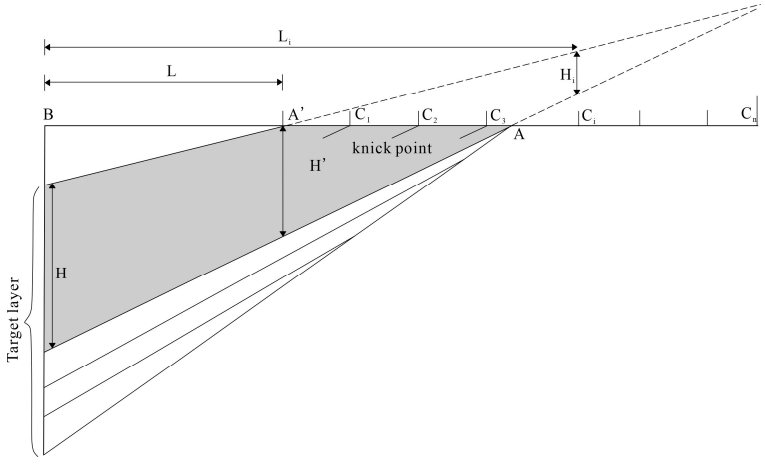


Figure 8. Schematic diagram of the principle of calculating denudation thickness using the stratigraphic trend extrapolation method.

The specific process for denudation restoration calculations is as follows:

Step One: Precisely locate two denudation reference points, A and A′, within the sedimentary layers. Given the constraints of seismic profile lengths, the exact denudation points may not always be identifiable. Consequently, the reference points selected are generally the apparent denudation points A′ and A, which are positioned closest to the basin's center on the profile [62].

Step Two: Compute the thinning rate K. This is achieved by identifying a strata segment (BA′) that exhibits a relatively stable thickness change towards the basin from the apparent denudation reference point A′. Designate the distance between BA′ as L and the apparent thickness of the strata segment at points A′ and B as H' and H, respectively. With these values, the thinning rate K can be derived using Equation (1).

$$K = (H - H')/L \times 100\%. \quad (1)$$

Step Three: Ascertain the pristine thickness of the strata, denoted as H_{i}. Commencing from the apparent denudation reference point A′, delineate the calculation points C_1, C_2, C_3, ..., C_{n} across the eroded region and ascertain the respective distances from these points to point B, labeled as L_1, L_2, L_3, ..., L_{n}. By applying Equation (2), one can deduce the original thickness of the strata at each designated point.

$$H_{\mathrm{i}} = H - K \times L_{\mathrm{i}}. \quad (2)$$

In this context, i equals 1, 2, 3,...,n.

Step Four: Calculate the denudation thickness, H_{b}. By subtracting the remaining strata thickness (h_{i}) from the original strata thickness (H_{i}) at each point, the denudation thickness (H_{b}) at each point can be determined. Formula (3) is as follows:

$$H_{\mathrm{b}} = H_{\mathrm{i}} - h_{\mathrm{i}}. \quad (3)$$

Step Five: Determine the actual thickness of the eroded strata. With the aid of the thinning rate K, the angle θ can be calculated as follows:

$$\theta = \mathrm{arctg}K = \mathrm{arctg}\left[(H - H')/L_i\right]. \quad (4)$$

Given the apparent thickness of the strata, the true thickness of the eroded strata, denoted as H_z, can be derived as follows:

$$H_{\mathrm{z}} = H_{\mathrm{i}} \times \cos\theta \quad (5)$$

Under the assumption of a consistent change in strata thickness, we can determine the depositional thinning rate, K, for the study section by utilizing the geophysical imaging attributes of the overlying strata from the regional seismic data within the research area. This enables us to estimate the original depositional thickness of the stratigraphic interval in question.

As the Changling Graben represents a classic graben basin, the original thickness of the strata deposited during the graben period is influenced by the faulting within the basin's depression. The strata attain their maximum thickness at the fault's root and thin in a wedge-like way from it. By leveraging the regional tectonic features and the characteristics of strata deposition, we apply the stratigraphic trend extrapolation method mentioned earlier, combined with a comprehensive tectonic–sedimentary strata approach. This integrated method accounts for the interplay between tectonics and sedimentation, as well as the effects of tectonic activity on denudation, thereby elucidating the dynamics of denudation. By steering clear of a purely trend-based extension and embracing the control of tectonic–sedimentary processes, we significantly reduce the margin of human error in our assessments. Consequently, this approach bolsters the precision of our estimates for the volume of denudation.

4. Results

4.1. Restoration Results of Graben Denudation in Changling Formation

Using the stratigraphic trend method, we have successfully reconstructed the denudation volumes for the four main tectonically active phases within the Changling Graben. As illustrated by the denudation volume restoration of the Shahezi Formation in the Changling

Graben (Figure 9), the denudation characteristics of the strata exhibit a clear pattern. By analyzing the underlying strata, their internal co-phase axes, and the strata's diminishing trend, and integrating these observations with the stratigraphic trend extrapolation method, we have been able to restore the denudation thickness across various strata. This approach not only restores the denudation thickness but also reinforces the theoretical foundation of the stratigraphic trend extrapolation method, which transitions from individual points to lines and ultimately to a comprehensive surface analysis.

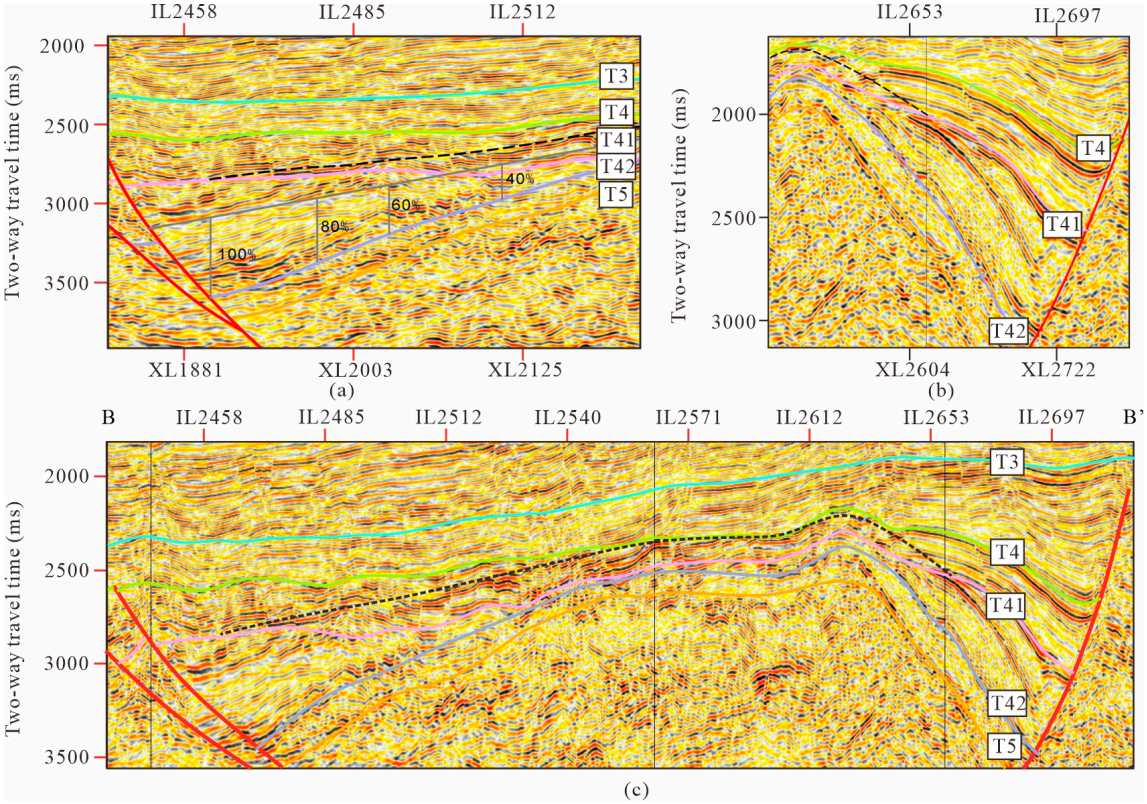


Figure 9. Denudation calculation of the Shahezi Formation in Changling Graben using the stratigraphic trend extrapolation method. Notes: (**a**) fold denudation type; (**b**) marginal uplift denudation type; (**c**) the location of the typical profile for denudation recovery is shown in (B,B').

Through the detailed restoration of the upper surfaces of each eroded stratum within the profile, it has been observed that the primary denudation in the study area occurred within the Huoshiling, Shahezi, and Yingcheng Formations, while the denudation thickness significantly decreased in the Denglouku Formation. By integrating the analysis of tectonic movements and regional context, we have achieved a comprehensive denudation restoration across the entire region, systematically transitioning from point to line and then to surface, thereby achieving a three-dimensional closure. This approach has allowed us to meticulously restore the denudation volumes for the Huoshiling, Shahezi, Yingcheng, and Denglouku Formations with a 16 × 16 grid density, as illustrated in Figure 9. Consequently, we have been able to estimate the denudation and the original depositional thickness data for the graben strata with greater precision.

(1) Denudation characteristics of Huoshiling Formation

Seismic profiles clearly reveal the most significant truncation characteristics in the central and northern sectors of the Changling Graben (Figure 10a). The stratigraphic distribution of the Huoshiling Formation is controlled by the boundary faults that define the depression, thereby establishing the fundamental structural framework of the graben basin. In the later stages of sedimentation, the strata experienced uplift due to tectonic

activities, followed by denudation, resulting in an angular unconformity with the overlying strata. Using the stratigraphic trend extrapolation method, we have determined that the denudation thickness across the Huoshiling Formation ranges from 0 to 450 m, with an average thickness of approximately 125 m. The most substantial denudation thickness is observed near the Shenzijing and Hashituo Troughs within the Changling Graben, with the central trough being the most severely eroded. In contrast, the northern and southern troughs exhibit relatively milder denudation and more intact strata. The residual thickness of the Huoshiling Formation varies from 0 to 1200 m, with the most significant denudation, around 417 m, noted in the Shenzijing–Hashituo region. The denudation intensity is most pronounced in the central region, decreasing from north to south, and the denudation thickness primarily extends in a north–south orientation.

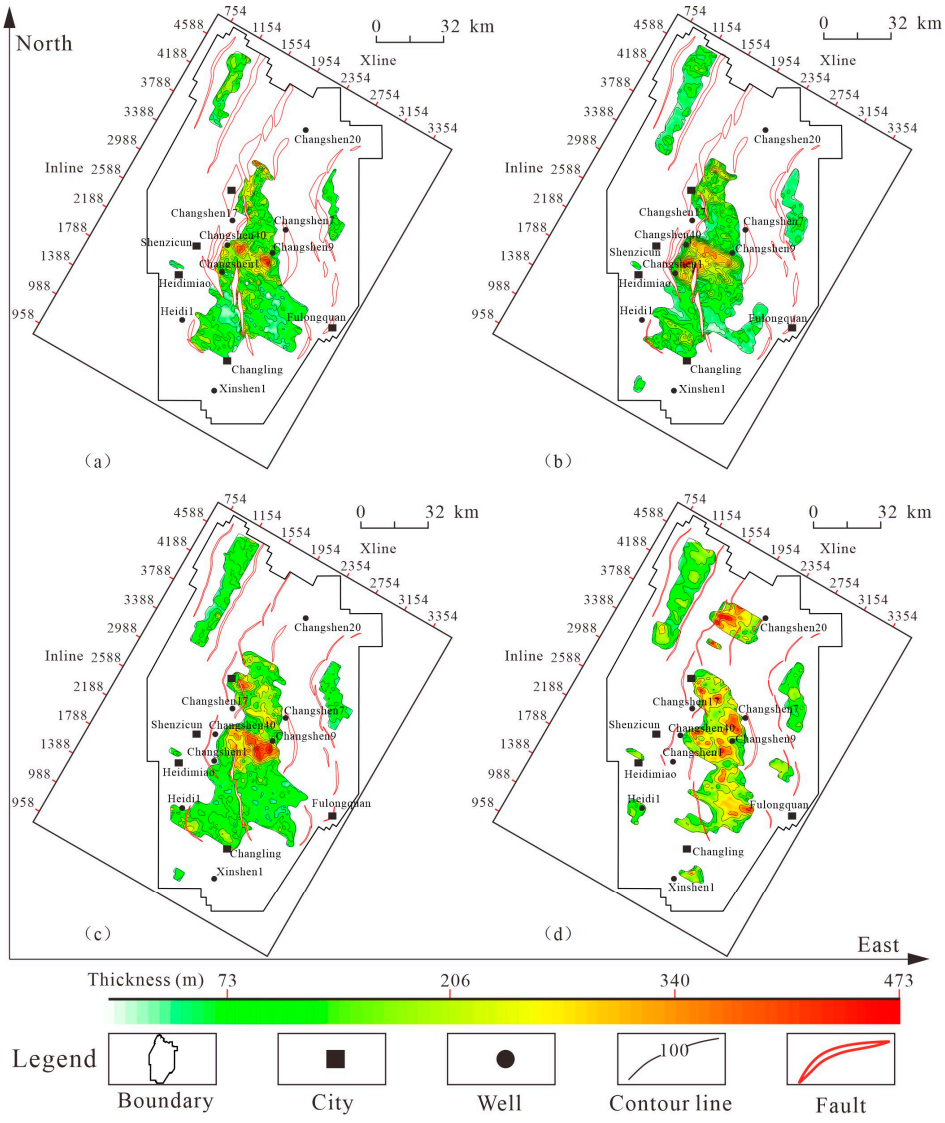


Figure 10. Denudation thickness map of the Huoshiling–Denglouku Formation in Changling Graben. Notes: (**a**) Huoshiling Formation; (**b**) Shahezi Formation; (**c**) Yingcheng Formation; (**d**) Denglouku Formation.

(2) Denudation characteristics of Shahezizu Formation

The denudation of the Shahezi Formation is predominantly evident in the regions of Shenzijing, Hashituo, Chaganhua, Fulongquan Troughs, and Da'an Graben, as depicted in Figure 10b. This formation experiences the most substantial denudation among the four targeted strata, with the remaining strata thickness varying from 0 to 1800 m across the

area. The denudation thickness within the Shahezi Formation itself spans from 0 to 750 m, with an average thickness of approximately 300 m.

Shaped by the faulting patterns of the depression, the strata from the graben period have evolved in a continuous sequence, yet the extent of denudation varies significantly across the basin's regions. The central trough experiences the most intense denudation. Analysis of the denudation characteristics of both the Huoshiling and Shahezi Formations indicates that during the Shahezi Formation's depositional phase, the Shenzijing and Hashituo areas were part of a symmetrical dual-fault structure, which initially formed a unified lake basin. This basin was later segmented by compressive tectonic forces towards the end of the Shahezi period, leading to extensive denudation. The residual thickness of the Huoshiling Formation ranges from 0 to 1200 m, with the most significant denudation, estimated at around 417 m, occurring in the Shenzijing–Hashituo region. The denudation intensity is most pronounced in the central areas, tapering from north to south, with the denudation thickness primarily oriented in a north–south direction.

(3) Denudation characteristics of Yingcheng Formation

The eroded strata of the Yingcheng Formation exhibit a thickness range from 0 to 450 m, with an average of approximately 100 m (as shown in Figure 10c). The overall pattern of denudation is similar to that observed in the Huoshiling and Shahezi Formations, with the central trough undergoing the most severe denudation. Notably, the degree of denudation in the Qianbei Trough has increased compared to the earlier two periods. The thickness of the remaining strata ranges from 0 to 2400 m.

(4) Denudation characteristics of Dengluoku Formation

The eroded strata of the Denglouku Formation exhibit a thickness range from 0 to 280 m, with an average thickness of approximately 120 m (as illustrated in Figure 10d). Within the Qianbei Trough, the erosive forces during the Denglouku epoch were significantly intensified. This epoch is characterized by a more distinct overall uplift, which has led to a significant broadening of the denudation boundaries across the basin. Despite this, the total denudation within the basin remains comparatively modest. The Denglouku Formation signifies a pivotal transition from a fault depression to an uplift phase, and by the conclusion of the Denglouku depositional period, a tectonic inversion event took place, causing a surge in denudation along both the eastern and western flanks.

The stratigraphic trend extrapolation method offers the advantages of speed and intuitiveness in denudation restoration, enabling the reconstruction of stratigraphic modifications caused by multiple denudation events. Through the analysis of denudation amounts across four periods, it was found that the denudation amounts ranged between 0 and 750 m, with an average of approximately 161 m. The Shenzijing–Hashituo sag area experienced the most intense denudation. However, there are potential uncertainties in the denudation restoration process, such as limitations in seismic data resolution. In this study, the latest 3D seismic data with good imaging quality and clear reflection features were collected to minimize errors caused by resolution limitations. Over long timescales, sea-level changes can significantly affect the deposition–denudation balance, leading to cumulative errors. By analyzing the regional geological background and sedimentary facies maps, it was determined that the water depth in the Changling Graben was approximately 40 m, corresponding to a residual thickness of about 2200 m, resulting in a paleo-water depth error impact of about 1.8%. Additionally, the dynamic coupling of tectonic activity and sedimentary environments may alter the original stratigraphic distribution patterns. This study integrated tectonic–sedimentary responses to minimize human cognitive errors as much as possible, enhancing the credibility of the research results.

The structural characteristics and distribution of denudation thickness within the Changling Graben demonstrate a distinct inheritability in the faults that have evolved across

different periods. The principal faults, which are long-term syndepositional and control the scale of development in various troughs, have directed the denudation range to evolve inherently from the base upwards. The Shenzijing and Hashituo regions stand out as the main denudation areas, with the Shahezi Formation recording the peak denudation values. The Yingcheng Formation exhibits a generally elevated degree of denudation, implying that the late-stage inversion and compression during the Yingcheng epoch were particularly forceful, impacting a substantial portion of the study area and resulting in a considerable uplift range. As we progress to the Denglouku Formation, denudation is notably reduced, yet the spatial extent of denudation expands, suggesting that the compressional stress during the Denglouku period was comparatively weaker. The concentration of denudation on the eastern side points to a more pronounced effect of compressive stress in this region, which also explains the greater uplift on the eastern side compared to the western side due to compressional forces. Moreover, the extent of denudation demonstrates an inverse relationship with fault scale: larger faults have a broader impact, while the influence of smaller faults is more limited, to the extent that their effect can be largely overlooked.

4.2. Seismic Response Characteristics of Sedimentary Facies

By integrating existing geological survey data and conducting comprehensive analyses of well logging, logging while drilling, and seismic profiles, we have developed a depositional facies model for the study area that includes four primary rock facies types: lacustrine, braided river delta, fan delta, and volcanic. The lacustrine facies acts as a significant background depositional facies in the Changling Graben, with seismic characteristics primarily displayed as parallel or sub-parallel, sheet-like reflection structures. The braided river delta facies is predominantly found on the gentle short-axis slopes or the narrow long-axis flanks of the graben, and its seismic response is marked by prograding, hummocky, or sheet-like reflection structures. The fan delta facies mainly develops along the side of the controlling depression fault, with seismic signatures typically presenting as hummocky wedge-shaped or discontinuous hummocky hill-shaped reflection structures. The volcanic facies, widely distributed within the Huoshiling and Yingcheng formations, often exhibit distinct arched, cone-shaped chaotic reflection structures on seismic profiles.

By integrating the distribution of denudation and sedimentary facies analysis (Figure 11) and using the depositional period of the Shahezi Formation as a case study, it is evident that the basin's structure during this era was profoundly influenced by the boundary fault-controlled depression. Intense graben activity resulted in the formation of multiple lake basins within the Changling Graben, which are classified as key background sedimentary facies of the Graben period. These can be categorized into marginal shallow lake, semi-deep lake, and deep lake subfacies. Driven by sediment supply from the Gudian Uplift and Shenzijing Uplift, small-scale fan delta deposits formed along the fault sides of each subordinate graben lake basin, transitioning to marginal shallow lake deposits towards the lake centers. The gentle short-axis slope of the Gudian Graben fostered the development of a braided river facies. Except for the central Trough, which extends continuously from Qianbei to Shenzijing to Chaganhua Trough, all other subordinate Troughs are distinctly segmented, creating a characteristic pattern of alternating depressions and uplifts [19,20]. Aligning with the denudation range, the differential uplift and subsidence of strata on either side of the controlling fault caused the upper plate strata to rapidly subside, accepting sedimentation, and leading the graben to evolve from initial compensation sedimentation to under-compensation sedimentation. This transition resulted in the deepening of water bodies and a swift shift to semi-deep to deep lake environments, triggering stratal onlap phenomena. Fan delta and braided river delta sand bodies developed on the steep and gentle slopes of the trough, respectively. Towards the end of the

Shahezi Formation's depositional period, the basin transitioned into a rapid graben phase, marked by localized compression, uplift, and denudation, predominantly within the semi-deep to deep lake zones. Denudation intensified from the depositional center outwards, peaking on the slopes and then gradually diminishing. This pattern corresponds to areas where under-compensation sedimentation was succeeded by compressional uplift and denudation. The reconstructed outcomes, synthesized from lithological and seismic facies data, align with the sedimentary facies, thereby validating the precision of the denudation volume restoration.

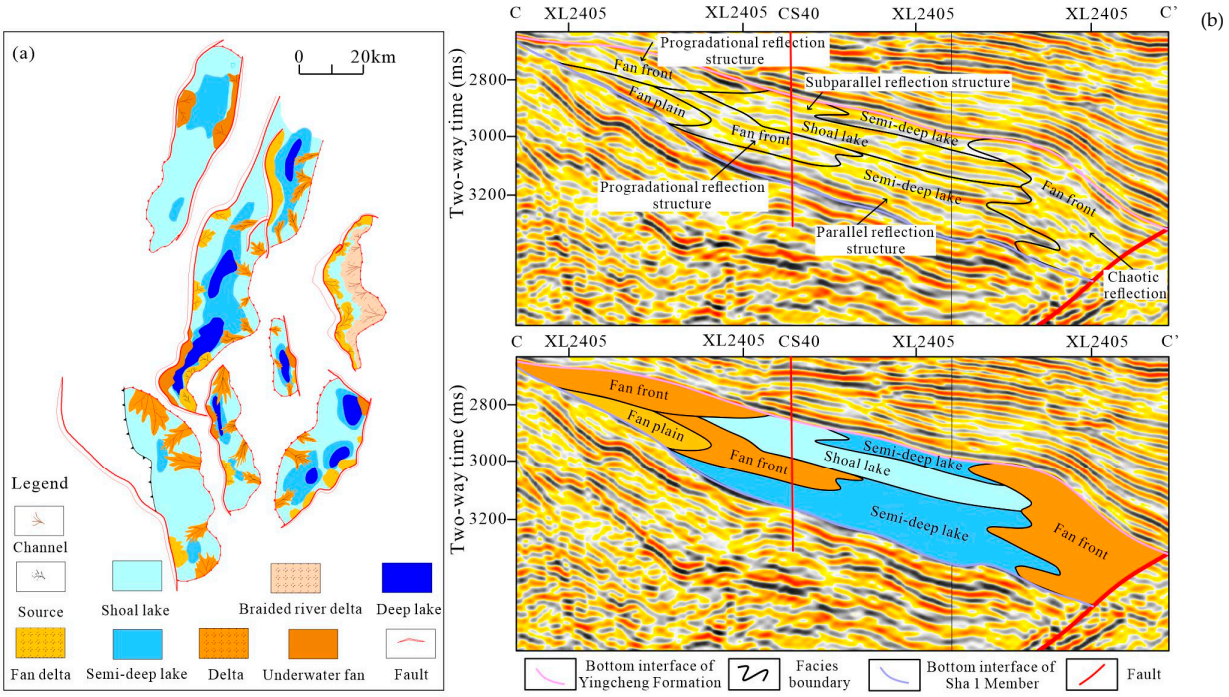


Figure 11. (**a**) Sedimentary facies map of the Shahezi Formation in Changling Graben; (**b**) interpretive seismic sedimentary facies profile of the Shahezi Formation in Changling Graben (see Figure 1 for profile location).

5. Discussion

Drawing on the calculated denudation thickness and its spatial distribution, in conjunction with the remaining strata thickness, we can deduce the original thickness of the strata. This foundation allows us to connect the evolution of geological structures with that of the strata and to correlate these denudation events with the principal tectonic activity periods within the basin, thereby establishing a link between tectonics and the evolution of troughs. This process aids in the reconstruction of the graben basin's original form. By integrating the regional geological context with an analysis of sedimentary facies, it was found that the maximum water depth in the Changling Graben was around 40 m, associated with a residual thickness of approximately 2200 m. The error impact on paleotopography is estimated to be about 1.8%. Therefore, this study has not included an analysis of paleowater depth. Instead, geological modeling techniques are utilized to reconstruct the paleotopography of the basin across various periods and are contrasted with current structural configurations. This comparison enables a more profound examination of the paleotectonic setup and the evolutionary history of the basin's prototype.

5.1. Analysis of Basin Tectonic Evolution

(1) Basin structure and sedimentary formation filling characteristics

Initial Stage of Graben—Huoshiling Formation Deposition: The remaining strata of the Huoshiling Formation reveal that the Changling Graben is composed of multiple independent residual depression groups, with individual grabens being relatively small in scale. During this period, the Shenzijing and Fulongquan areas exhibit the maximum depositional thickness and rate, with intense deposition concentrated in the central region, gradually decreasing towards the north and south.

Intense Stage of Graben—Shahezi–Yingcheng Formation Deposition: During the Shahezi Formation depositional period, compared to the Huoshiling Formation, the scale of the Qianbei Trough expanded. In the Yingcheng Formation period, faults and strata acted simultaneously to promote the further development and strengthening of each subordinate graben, with significant tectonic subsidence in the Heidimiao area during this period. The depositional thickness and rate at this time show a pattern of weaker in the south and stronger in the north, indicating a northward shift in the depositional center compared to the Huoshiling period.

Transition from Fault Depression to Uplift—Denglouku Formation Deposition: During this period, the strata underwent non-uniform subsidence, and by the end of this period, some grabens experienced tectonic inversion, leading to denudation on the eastern and western sides. The basin began to subside, and the depositional range started to expand, gradually evolving into a unified large depression lake basin, marking the initial stage of the Songliao Basin's subsidence. At this time, the Qianbei area exhibited strong deposition, while the Heidimiao area experienced relatively strong deposition. In contrast, the depositional thickness and rate in the Shenzijing area during the Denglouku period were notably weak. This reflects the controlling influence of the structural deformation differences in the Changling Graben on the thickness and rate of depositional strata.

(2) Basin tectonic evolution

Based on the geological background of the Changling Graben area, the characteristics of basin sedimentation and filling, and the patterns of geological structures, combined with the research findings of previous studies, the tectonic evolution of the Changling Graben is divided into three stages(Figure 12): the graben stage, the sag stage, and the inversion stage. This study adheres to the principle of cutting through the main tectonic units with key profiles, dividing them into five representative horizontal and three vertical structural framework profiles. Through the analysis of the basin's structural framework, it is determined that the Changling Graben has a characteristic structure of being divided into eastern and western zones and northern and southern sections. This study selects the profile passing through the Shenzijing, Hashituo, and Fulongquan areas as a typical profile. By integrating regional geological background analysis, seismic profile structural interpretation, regional unconformities, and the restoration of denudation volumes, the tectonic evolution process of the Changling Graben is analyzed.

The Huoshiling-Yingcheng Formation period (145 Ma–124 Ma) represents the graben stage. During the depositional period of the Huoshiling Formation, following the formation of the basin's base, the basin experienced NNW-directed compression from the Izanagi Plate to the east, accompanied by large-scale volcanic activity. This led to the formation of several NNE- and NNW-oriented major faults within the basin. These faults have distinct graben and half-graben structural forms, laying the foundation for the later development of the graben and initially forming the basic structural pattern of the graben basin. At the end of the Huoshiling depositional period, fault activity weakened, the strata were uplifted as a whole, and the shrinkage of the lake basin at the end of the deposition led to extensive denudation of the early-deposited Huoshiling Formation in the Changling Graben, resulting in an angular unconformity with the overlying strata. During the Shahezi–Yingcheng Formation depositional period, the controlling depression faults continued to be

active, governing the deposition and development of the strata, which mainly developed in the sag on the downthrown side of the faults. The strata were thickest at the fault roots and wedged out away from the faults. In the Shenzijing Trough, it manifests as the stage of filling and compensation. At the end of the graben period, tectonic inversion occurred; the strata were uplifted and eroded, forming an unconformity interface.

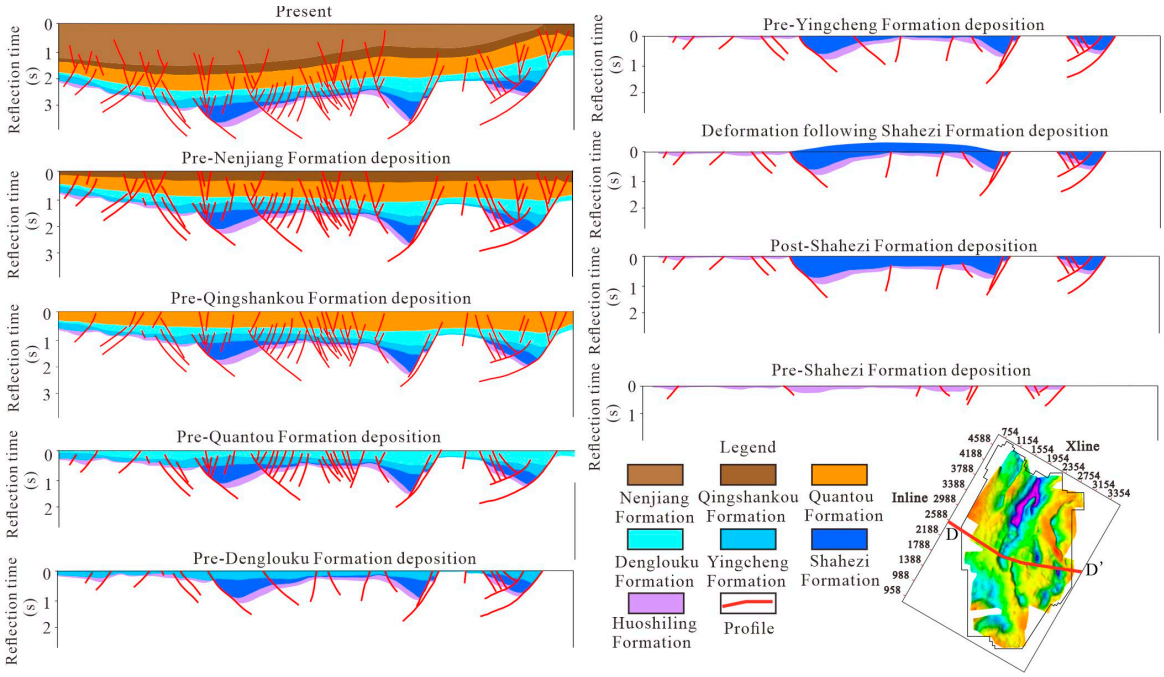


Figure 12. Results of structural evolution restoration of the typical profile in Changling Graben.

During the Denglouku Formation's (124 Ma–112 Ma) depositional epoch, which signifies the shift from fault-controlled depression to sag, the basin collectively entered a phase characterized by sag subsidence. The robust tectonic inversion and crustal uplift that marked the conclusion of the Yingcheng Formation's deposition evolved into a period of relaxation and elongation. The early continued activity of the controlling depression faults led to non-uniform crustal subsidence, with the strata beneath the Denglouku Formation being notably influenced by fault control, displaying graben traits [63]. However, Denglouku's subsidence area is significantly more expansive than the underlying graben layers, also reflecting sag features. Towards the end of the Denglouku Formation's deposition, certain grabens experienced tectonic inversion, with denudation affecting the eastern and western flanks. The basin commenced sinking, its depositional range broadened, and it progressively transformed into a cohesive large depression lake basin, thereby heralding the commencement of the Songliao Basin's sag phase.

The Quantou–Nenjiang Formation's depositional interval marks the sag phase, characterized by widespread blanket sedimentation that extended across the entire region, connecting various troughs and showcasing a distinct, unified stratigraphic distribution pattern. At the end of the Nenjiang Formation's deposition, compressive folding movements occurred, with the graben's controlling faults reversing and thrusting, forming low-amplitude, broad-fold structures. However, during this period, inversion structures were minimal in the Shenzijing–Hashituo areas of the Changling Graben, with only slight stratal flexures evident near the principal controlling faults, suggesting a generally subdued degree of deformation.

As the deposition of the Nenjiang Formation neared its end, the basin began a gradual contraction, entering the inversion phase, which coincided with the late-stage tectonic

inversion of the Songliao Basin. During this period, the Changling Graben also experienced regional tectonic inversion. Additionally, extensional activities were present, giving rise to a modest number of normal faults that interconnected segmentally with the underlying faults. This resulted in more substantial displacements in the upper sections and comparatively minor ones in the lower sections.

5.2. Analysis of Paleogeomorphic Features of Basin

During the Huoshiling Formation epoch (Figure 13a), the Changling Graben was characterized by low-amplitude, scattered troughs, with the more significant ones located along the central and eastern trough belts. The basin's prototype at this time exhibited a classic graben structure, featuring a pattern of alternating depressions and uplifts, with the Shenzijing Trough as the central subsidence point and a notably high sedimentation rate.

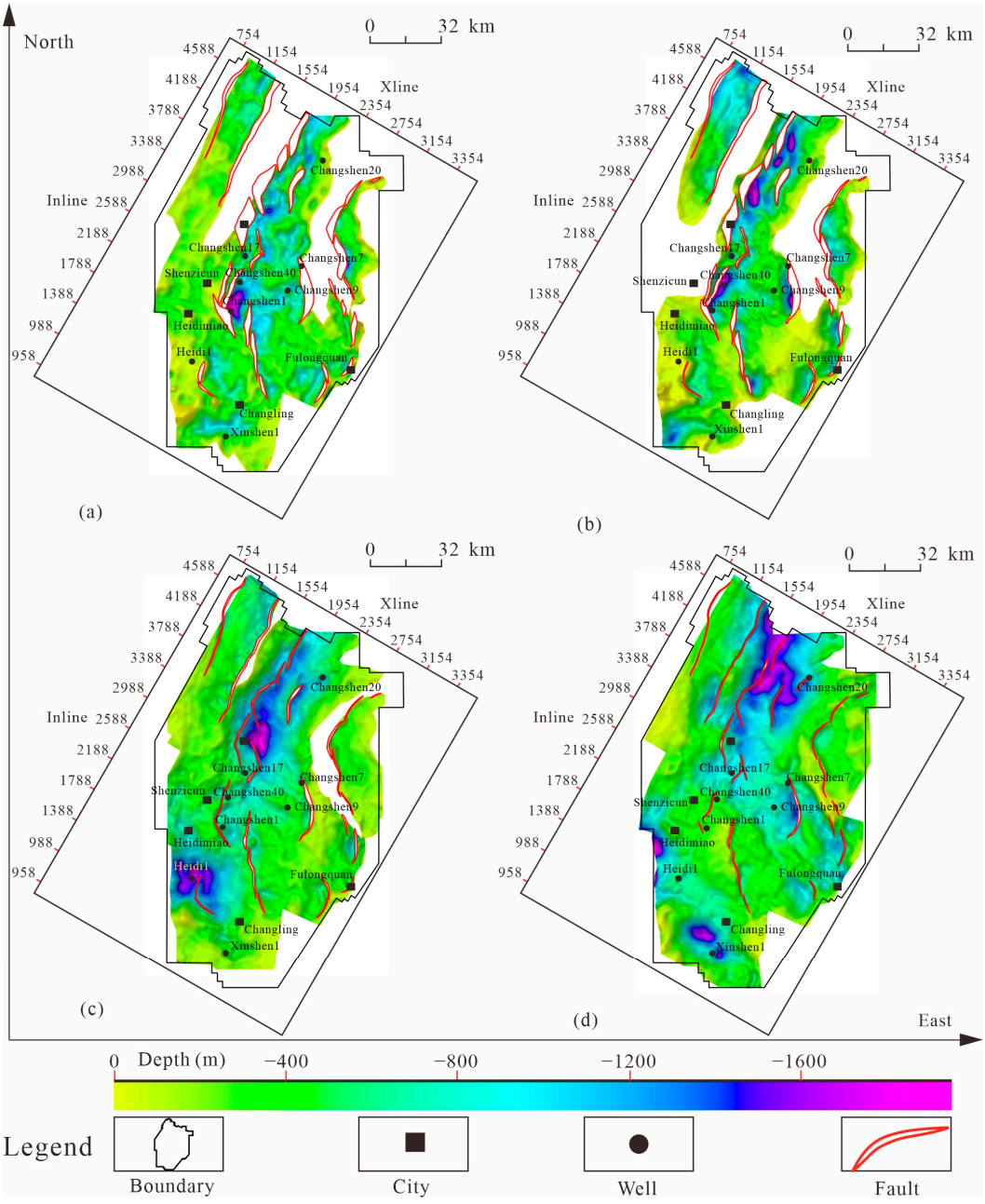


Figure 13. Protolithic basin of the Huoshiling–Denglouku Formation in Changling Graben. Notes: (**a**) Huoshiling Formation; (**b**) Shahezi Formation; (**c**) Yingcheng Formation; (**d**) Denglouku Formation.

As the Shahezi Formation period progressed (Figure 13b), the impact of tectonic uplift transformed the previously scattered small troughs into more expansive regional troughs. Notable examples include the Heidimiao Trough in the southwest, the Qianbei Trough in the center, the Shenzijing Trough, the Hashituo Trough, and the Fulongquan Trough in the southeast, effectively defining the distribution range of Troughs within the Changling Graben. The general low-lying paleotopographic areas were concentrated in the central band of the Changling Graben, indicating that the primary subsidence region during the Shahezi period was likely centered on the Qianbei–Shenzijing–Chaganhua–Hashituo axis [64].

During the Yingcheng Formation period (Figure 13c), troughs were mainly located in the Qianbei Trough and the Heidimiao–Longfengshan Trough, while the paleotopography of the Da'an Graben, Fulongquan, and Gudian Trough was relatively higher. The slope development areas for the Yingcheng Formation were identified in the southern part of the Da'an Graben, along the eastern and western flanks of the Qianbei Trough, between Chaganhua and Hashituo, in the eastern portion of the Gudian Graben, and in the southern reaches of the Heidimiao Trough. The regions experiencing rapid subsidence and significant deposition in the Changling Graben at this time were primarily concentrated in the Qianbei Trough and the Heidimiao–Longfengshan Trough.

During the Denglouku Formation period (Figure 13d), troughs were primarily distributed across the Qianbei–Shenzijing northern part, Hashituo Trough, Heidimiao, and Longfengshan Trough. The area between Shenzijing–Chaganhua and Fulongquan stood as a high paleotopographic area, while other areas were characterized as slope zones. Throughout this period, the paleotopographic troughs, slopes, and uplifts in the Changling Graben developed in tandem.

The structural analysis of the Changling Graben's prototypical basin (as illustrated in Figure 13) reveals a strong inheritability in the development of troughs throughout the graben phase. The Qianbei Trough, which has consistently served as a tectonic subsidence center since the Huoshiling Formation's depositional phase, stands out as the most deeply incised structural trough on an extensive scale. During the Huoshiling period, the epicenters of subsidence were located in the Shenzijing and Fulongquan areas. Subsidence in the Qianbei area began to intensify from the Shahezi period, reaching its peak during the Yingcheng period, with Qianbei being the most significant and Heidimiao being the secondary center. By the Denglouku period, the Qianbei area had become a robust subsidence zone, while Heidimiao maintained a stable, albeit weaker, subsidence pattern.

In the early stages of the tectonic graben, the Shenzijing area was notably active, with the Shenzijing Trough transitioning from a deep to a shallow configuration from the Huoshiling to the Denglouku period. This shift indicates a gradual decline in tectonic subsidence at the Shenzijing Trough over time. In the later stages, the Qianbei area exhibited strong activity. Stratigraphically, this is reflected in the thickness variations, with the Shenzijing area displaying thick deposits in the early stages and thinner layers in the later stages, while the Qianbei area showed the opposite pattern [33,34]. The Heidimiao Trough's depth at the base of the Yingcheng Formation indicates substantial tectonic subsidence during that era.

The lateral sedimentary centers of the Changling Graben exhibit a northward migration from early to late periods. The prototypical basin formed during the Huoshiling Formation established the foundational structural framework of the Changling Graben, with the central subsidence area shifting from the Shenzijing Trough in the early stages to the northern Qianbei Trough. During the Denglouku depositional phase, the basin gradually evolved into a cohesive, large depression lake basin, characterized by widespread blanket sedimentation across the entire region [65]. This evolution outlines a longitudinal

trend from graben to sag to inversion, essentially mapping out the basin-formation journey of the Changling Graben.

By synthesizing the evolutionary trajectories of each trough, the Changling Graben can be categorized into two models comprising three types of Troughs: the "inversion-type" troughs that begin with intense rifting, followed by a subdued graben phase, and culminate in inversion, such as the Shenzijing Trough, Chaganhua Trough, and Gudian Graben; the "inversion-type" troughs that start with a weaker phase, evolve into a robust graben, and conclude with inversion, like the Heidimiao Trough, Longfengshan Trough, Da'an Graben, Hashituo Trough, and Fulongquan Graben; and the "inherited-type" Troughs that begin with a weaker phase, strengthen in the middle Graben phase, and maintain their intensity in the later stages, exemplified by the Qianbei Trough.

6. Conclusions

(1) The denudation volume restoration of the graben strata within the Changling Graben reveals an inheritable expansion of denudation from the base upwards, strongly influenced by faulting, with the most intense denudation occurring in the central regions. The denudation thickness data indicate that the Shahezi Formation undergoes the most significant denudation, while the Yingcheng Formation exhibits a consistently high degree of denudation. This suggests a period of pronounced structural inversion after the Shahezi–Yingcheng depositional phase, characterized by substantial uplift and denudation of the strata.

(2) The protolithic basin restoration of the Changling Graben reveals that the Huoshiling Formation exhibits its maximum depositional thickness and rate in the Shenzijing and Fulongquan areas, with deposition intensity decreasing towards the north and south. During the Shahezi period, the depositional thickness and rate show a gradient that is weaker in the south and stronger in the north. In the case of the Yingcheng–Denglouku Formations, the basin transitioned into a subsidence phase, characterized by an expanded sedimentation range, with a notably high deposition rate in the Qianbei and Heidimiao areas during the Denglouku period. In contrast, the depositional thickness and rate in the Shenzijing area during the Denglouku period are significantly reduced, confirming the temporal migration of the lateral subsidence center from south to north.

(3) The troughs within the graben period exhibit a distinct inheritable developmental pattern, with faults demonstrating clear inheritability across different periods, thereby governing the scale of development for each trough. Strata beneath the Denglouku Formation are strongly influenced by fault control, displaying characteristics of a graben. Following the deposition of the Denglouku Formation, the basin transitioned into a subsidence phase, characterized by a significantly broader sedimentation range compared to the underlying graben, illustrating a vertical evolutionary trajectory from early graben formation through subsidence to eventual inversion.

Author Contributions: J.Z. was involved in data statistical analysis and manuscript writing; T.L. participated in project supervision and guidance; J.H. provided geological data support; H.W. was involved in data organization; T.Y. participated in data statistical analysis; J.L. provided technical support; Y.C. was involved in data analysis. All authors have read and agreed to the published version of the manuscript.

Funding: This research was funded by the Jilin Oilfield Branch of China National Petroleum Corporation, Research Institute of Geophysical Exploration and Development Project (JLYT-ZBZX-2021-FW-128).

Institutional Review Board Statement: Not applicable.

Informed Consent Statement: Not applicable.

Data Availability Statement: Data is contained within the article.

Conflicts of Interest: Author Jia Hu was employed by the company PetroChina Jilin Oilfield Company, and Hui Wang was employed by the company Exploration and Development Research Institute of Daqing Oilfield Co., Ltd. The remaining authors declare that the research was conducted in the absence of any commercial or financial relationships that could be construed as a potential conflict of interest.

References

1. Liu, X.; Zhong, J.; Grapes, R.; Bian, S.; Liang, C. Late cretaceous tempestite in northern songliao basin, China. *J. Asian Earth Sci.* **2012**, *56*, 33–41. [CrossRef]
2. Liu, C.; Fu, X.; Li, Y.; Wang, H.; Sun, L.; Lu, J.; Li, J.; Sun, Y.; Shi, L.; Hu, H.; et al. Petroleum exploration breakthrough and geological significance in cretaceous yingcheng and denglouku formations of shuangcheng area, northern songliao basin, ne china. *Pet. Explor. Dev.* **2023**, *50*, 72–84. [CrossRef]
3. Ma, L. Subtle oil pools in xingshugang delta, songliao basin. *AAPG Bull. Am. Assoc. Pet. Geol.* **1985**, *69*, 1123–1132.
4. Li, Z.; Kusky, T.; Ying, D.; Guo, X.; Li, H. Successor characteristics of the mesozoic and cenozoic songliao basins. *Acta Geol. Sin. Engl. Ed.* **2008**, *82*, 622–628.
5. Wan, X.; Zhao, J.; Scott, R.W.; Wang, P.; Feng, Z.; Huang, Q.; Xi, D. Late cretaceous stratigraphy, songliao basin, ne china: Sk1 cores. *Palaeogeogr. Palaeoclimatol. Palaeoecol.* **2013**, *385*, 31–43. [CrossRef]
6. Anees, A.; Zhang, H.; Ashraf, U.; Zhang, X.; Duan, L. Structural styles and impact of fault subsidence in the lake fuxian basin and adjacent area. *Mar. Geophys. Res.* **2024**, *45*, 11. [CrossRef]
7. Dou, L.; Wen, Z. Classification and exploration potential of sedimentary basins based on the superposition and evolution process of prototype basins. *Pet. Explor. Dev.* **2021**, *48*, 1271–1288. [CrossRef]
8. Chen, Z.; Guo, Q.; Liu, H. The evolution of prototype basin and its relation to sandstone-hosted uranium ore-formation in northwestern china. In Proceedings of the 8th Biennial SGA Meeting, Beijing, China, 18–21 August 2005; pp. 241–243.
9. Lou, Q.; Xiao, A.; Zhong, N.; Wu, L. A method of prototype restoration of large depressions with terrestrial sediments: A case study from the cenozoic qaidam basin. *Acta Petrol. Sin.* **2016**, *32*, 892–902.
10. Changqing, Y.; Yanqiu, Y.; Gang, L.; Chuansheng, Y.; Jinyu, Y. The mesozoic basin-mountain coupling process of the southern east china sea shelf basin and its adjacent land area. *Acta Geol. Sin. Engl. Ed.* **2016**, *90*, 1051–1052. [CrossRef]
11. Corrigan, J.; Cervany, P.F.; Donelick, R.; Bergman, S.C. Postorogenic denudation along the late paleozoic ouachita trend, south central united states of america: Magnitude and timing constraints from apatite fission track data. *Tectonics* **1998**, *17*, 587–603. [CrossRef]
12. Li, D.; Yang, S.; Chen, H.; Cheng, X.; Li, K.; Jin, X.; Li, Z.; Li, Y.; Zou, S. Late carboniferous crustal uplift of the tarim plate and its constraints on the evolution of the early permian tarim large igneous province. *Lithos* **2014**, *204*, 36–46. [CrossRef]
13. Liu, Z.; Peng, S.; Qin, M.; Huang, S.; Geng, Y.; He, Z. Constraints on sandstone-type uranium deposits by the tectonic uplift and denudation process in the eastern junggar basin, northwest china: Evidence from apatite fission track and detrital zircon u-pb ages. *Minerals* **2022**, *12*, 905. [CrossRef]
14. Li, G.; Zhong, Q.; Dian, L.; Liu, H.; Yan, S.; Su, G.; Tian, X. Continuous extensional uplift controls the silurian structural evolution of the sichuan basin, southwest china. *Mar. Pet. Geol.* **2023**, *155*, 106383. [CrossRef]
15. Serikov, G.; Zhuniskenov, Y.; Abbas, A.H.; Pourafshary, P. Synergistic application of Welan gum and polysaccharides for enhanced oil recovery. *J. Pet. Explor. Prod. Technol.* **2025**, *15*, 47. [CrossRef]
16. Luszczak, K.; Persano, C.; Braun, J.; Stuart, F.M. How local crustal thermal properties influence the amount of denudation derived from low-temperature thermochronometry. *Geology* **2017**, *45*, 779–782. [CrossRef]
17. Wang, Y.; Guoqiang, X.; Pang, X.; Zuo, Y.; Liu, B.; Han, J.; Chen, M.; Guo, W. A method for restoring sedimentary sequence original structural profiles: A case study of miocene strata from the northern continental slope of the south china sea. *Mar. Pet. Geol.* **2019**, *103*, 294–305. [CrossRef]
18. Otofuji, Y.-I. Estimating the amount of uplift from the current elevation of strata at the middle miocene climatic optimum: A case study of kibi plateau in southwest Japan. *Isl. Arc* **2024**, *33*, e12531. [CrossRef]
19. Yang, X.; Wang, H.; Li, Z.; Guan, C.; Wang, X. Tectonic-sedimentary evolution of a continental rift basin: A case study of the early cretaceous changling and lishu fault depressions, southern songliao basin, china. *Mar. Pet. Geol.* **2021**, *128*, 105068. [CrossRef]
20. Zhang, Z.; Wang, H.; Yang, X.; Su, X.; Tian, Y.; Wang, J.; Shi, N. Seismic interpretation and geological evaluation of hydrocarbon source rocks in volcanic-rich continental lacustrine rift basins: A case study of the lower cretaceous yingcheng formation from the changling fault depression in the songliao basin, ne China. *Geoenergy Sci. Eng.* **2023**, *221*, 211397. [CrossRef]
21. Rowley, E.; White, N. Inverse modelling of extension and denudation in the east Irish sea and surrounding areas. *Earth Planet. Sci. Lett.* **1998**, *161*, 57–71. [CrossRef]
22. Meckel, T.A.; ten Brink, U.S.; Williams, S.J. Current subsidence rates due to compaction of holocene sediments in southern louisiana. *Geophys. Res. Lett.* **2006**, *33*, 11. [CrossRef]

23. Suetnova, E.I. Influence of the fluid-dynamic and rheological properties of sediments on the process of viscoelastic compaction at different rates of sedimentation. *Izv. Phys. Solid Earth* **2010**, *46*, 529–537. [CrossRef]
24. Gioia, D.; Gallicchio, S.; Moretti, M.; Schiattarella, M. Landscape response to tectonic and climatic forcing in the foredeep of the southern Apennines, Italy: Insights from Quaternary stratigraphy, quantitative geomorphic analysis, and denudation rate proxies. *Earth Surf. Process. Landforms* **2014**, *39*, 814–835. [CrossRef]
25. Eriksson, K.A.; Romans, B.W. Denudation rates of a subequatorial orogenic belt based on estimates of sediment yields: Evidence from the paleozoic appalachian basin, USA. *Basin Res.* **2015**, *29*, 2–15. [CrossRef]
26. Müller, S.M.; Jähne-Klingberg, F.; Thöle, H.; Jakobsen, F.C.; Bense, F.; Winsemann, J.; Gaedicke, C. Jurassic to lower cretaceous tectonostratigraphy of the german central graben, southern north sea. *Neth. J. Geosci.* **2023**, *102*, e4. [CrossRef]
27. Yilmaz, Y.; Gürer, Ö.F.; Erbay, A.Y. Morphotectonic evolution of selcuk graben in development process of western anatolian grabens. *Turk. Jeol. Bul. Geol. Bull. Turk.* **2023**, *66*, 275–324. [CrossRef]
28. Yin, S.; Radwan, A.E.; Xiao, F.; Xie, G.; Lai, P. Developmental characteristics of vertical natural fracture in low-permeability oil sandstones and its influence on hydraulic fracture propagation. *Geomech. Geophys. Geo-Energy Geo-Resour.* **2024**, *10*, 165. [CrossRef]
29. Zhang, P.; Misch, D.; Meng, Q.; Sachsenhofer, R.F.; Liu, Z.; Jia, J.; Gao, F.; Bechtel, A.; Hu, F. Lateral changes of organic matter preservation in the lacustrine qingshankou formation (cretaceous songliao basin, ne china): Evidence for basin segmentation. *Int. J. Coal Geol.* **2022**, *254*, 103984. [CrossRef]
30. He, C.; Lin, Y.; Zhang, T.; Ma, J.; Li, Y.; Cheng, J.; Zhang, Y. Study on the structural characteristics of the yangdachengzi oil layer in the quantou formation, zy block, central depression, songliao basin. *Front. Earth Sci.* **2023**, *11*, 1132837. [CrossRef]
31. Zhang, X.; Zhu, L.; Wang, T.; Shi, X.; Han, B.; Shen, J.; Gao, H. Fluid property identification of the Lower Cretaceous reservoirs with complex oil-water contacts in Deseo Basin, Chad. *Energy Geosci.* **2023**, *5*, 100219. [CrossRef]
32. Yan, X.; Xue, H.T. Huoshiling formation volcanic reservoir control factors analysis of wangfu fault depression in southern songliao basin. In Proceedings of the 3rd International Conference on Energy, Environment and Sustainable Development (EESD 2013), Shanghai, China, 12–13 November 2013; pp. 101–106. [CrossRef]
33. Lou, R.; Wang, L.; Wang, L.; Yang, G.; Wang, J.; Liu, C.; Pei, Y.; Zhang, C. Characteristics of fluid inclusions and hydrocarbon accumulation period of huoshiling -yingcheng formations in wangfu fault depression, songliao basin, China. *J. Pet. Sci. Eng.* **2021**, *208*, 109421. [CrossRef]
34. Xu, L.; Wang, R.; Shi, W.; Yu, G.; Zhang, X.; Tang, D.; Meng, F. Characteristics and main controls of tectonic fractures and their contribution to deep tight reservoirs: A case study of the huoshiling-shahezi formations in gudian half-graben, songliao basin, China. *Lithosphere* **2022**, *2022*, 7168037. [CrossRef]
35. Shi, Y.; Yi, J.; Bian, W.; Shan, X.; Liu, Y.; Hao, G.; Li, A.; Leng, Q.; Lu, J.; Pang, H.; et al. Reservoir characteristics and development model of subaqueous pyroclastic rocks in a continental lacustrine basin: A case study of the chaganhua subsag in the changling fault depression, songliao basin. *Energies* **2023**, *16*, 4968. [CrossRef]
36. Liu, T.; Zhang, W.; Chen, C.; Shen, H.; Shao, W.; Sun, P. Controlling factors of fluid mobility in the tuff reservoirs of the huoshiling formation, dehui fault depression, southeastern songliao basin: Insights from micro-nano pore structures. *Front. Earth Sci.* **2024**, *12*, 1502160. [CrossRef]
37. Cui, J.; Zhu, R.; Wang, C.; Gao, Y.; Li, S.; Kang, L. Source/reservoir characteristics and shale gas "sweet spot" interval in shahezi mudstone of well skii in songliao basin, ne China. *Arab. J. Geosci.* **2020**, *13*, 514. [CrossRef]
38. Han, S.; Du, X.; He, Y.; Wang, C.; Huo, M.; Mu, X.; Wang, Y.; Huang, J.; Zhang, C. Sedimentary paleoenvironment and organic matter enrichment characteristics of lacustrine shahezi shale in songliao basin: Insights from the continental scientific drilling. *ACS Omega* **2024**, *9*, 21097–21115. [CrossRef]
39. Liu, D.; Li, Z.; Jiang, Z.; Zhang, C.; Zhang, Z.; Wang, J.; Yang, D.; Song, Y.; Luo, Q. Impact of laminae on pore structures of lacustrine shales in the southern songliao basin, ne China. *J. Asian Earth Sci.* **2019**, *182*, 103935. [CrossRef]
40. Yu, Z.; He, H.; Deng, C.; Lu, K.; Shen, Z.; Li, Q. New SIMS U-Pb geochronology for the Shahezi Formation from CCSD-SK-IIe borehole in the Songliao Basin, NE China. *Sci. Bull.* **2020**, *65*, 1049–1051. [CrossRef]
41. Xiao, D.; Lu, S.; Shao, M.; Zhou, N.; Zhao, R.; Peng, Y. Comparison of marine and continental shale gas reservoirs and their gas-bearing properties in China: The examples of the longmaxi and shahezi shales. *Energy Fuels* **2021**, *35*, 4029–4043. [CrossRef]
42. Li, Z.; Li, C.; Li, W.; Liu, Y. Evolution and characteristics of sedimentary systems during fault-depressed transition in songliao basin-case study of the denglouku formation in the southeast uplift region. *Indian J. Geo Mar. Sci.* **2018**, *47*, 2353–2368.
43. Li, Z.-D.; Wang, P.; Li, L.; Li, W.; Xu, J.-Z.; Liu, Y.-K. Study of sedimentary characteristic in Denglouku formation, southern Songliao basin, Northeast China. *Carbonates Evaporites* **2018**, *34*, 1141–1155. [CrossRef]
44. Zhang, X.J.; Zhang, L.; Yang, Z. RSeismic prediction method for dark mudstone thickness of the second member of the denglouku formation in northern songliao basin. In Proceedings of the 2nd International Conference on Energy, Environment and Sustainable Development (EESD 2012), Jilin, China, 12–14 October 2012; pp. 411–420. [CrossRef]

45. Liu, B.; Liu, L.; Fu, J.; Lin, T.; He, J.; Liu, X.; Liu, Y.; Fu, X. The songliao super basin in northeastern China. *AAPG Bull.* **2023**, *107*, 1257–1297. [CrossRef]
46. Wang, L.; Jin, Z.; Liu, Q.; Liu, K.; Meng, Q.; Huang, X.; Su, Y.; Zhang, Q. The occurrence pattern of natural hydrogen in the songliao basin, pr china: Insights on natural hydrogen exploration. *Int. J. Hydrogen Energy* **2023**, *50*, 261–275. [CrossRef]
47. Yi, J.; Sun, F.; Wang, P.; Shan, X. Vesicle distribution in acidic lava flow units in the rift basins of ne china: Implications for petroleum reservoir exploration. *Geol. J.* **2016**, *52*, 609–623. [CrossRef]
48. Li, M.; Yan, X.; Zhang, W.; Guo, Y.; Liu, C.; Fan, L.; Yang, S. Characteristics and genetic mechanism of the Mesoproterozoic rift system, Ordos Basin, China. *Energy Geosci.* **2024**, *5*, 100221. [CrossRef]
49. Zhang, L.; Liang, X.; Yang, W.; Xiao, C.; Zhang, J.; Wang, X.; Dai, R. Geothermal water boron enrichment patterns in the quantou formation, central depression of the southern songliao basin. *Geothermics* **2024**, *120*, 103016. [CrossRef]
50. Ashraf, U.; Zhang, H.; Anees, A.; Zhang, X.; Duan, L. Assessment of lake-level variations to decipher geological controlling factors and depositional architecture of lake fuxian, yunnan plateau: Preliminary insights from geophysical data. *Geomech. Geophys. Geo-Energy Geo-Resour.* **2024**, *10*, 64. [CrossRef]
51. Fossen, H.; Schultz, R.A.; Rundhovde, E.; Rotevatn, A.; Buckley, S.J. Fault linkage and graben stepovers in the canyonlands (utah) and the north sea viking graben, with implications for hydrocarbon migration and accumulation. *AAPG Bull.* **2010**, *94*, 597–613. [CrossRef]
52. Obi, I.S.; Onuoha, K.M.; Dim, C.I.P. Highlighting relationships between sand thicknesses, reservoir-seal pairs and paleobathymetry from a sequence stratigraphic perspective: An example from Tortonian Serravallian deposits, onshore Niger Delta Basin. *Energy Geosci.* **2023**, *5*, 100215. [CrossRef]
53. Li, P.; He, Z.; Hu, Z.; Zhang, Y.; Feng, J. Conditions for the enrichment of karst hydrothermal resources in Bohai Bay Basin. *Energy Geosci.* **2024**, *5*, 100234. [CrossRef]
54. Zhang, L. Denudation rates of crystalline rock in the huangling anticline of the three gorges of the yangtze river in china since the eocene. *Sci. China Ser. D Earth Sci.* **2003**, *46*, 928–940. [CrossRef]
55. Albaroot, M.; Elhossainy, M.M.; Al-Areeq, N.M.; Abdullah, E.A.; Salman, A.M. The Upper Jurassic sediments, Marib-Shabwa Basin, Yemen: Lithofacies aspects and sequence stratigraphic analysis. *Energy Geosci.* **2023**, *5*, 100214. [CrossRef]
56. Guo, Q.; Wang, X.; Yin, S.; Wu, Z. Tectonic evolution and gas control analysis of the upper palaeozoic tight sandstone reservoirs in the linxing area of the eastern ordos basin. *Geol. J.* **2021**, *56*, 1625–1637. [CrossRef]
57. Shi, S.; Wang, Y.; Chen, C.; Liu, J.; Peng, P. Influence of tectonic evolution processes on burial, thermal maturation and gas generation histories of the wufeng-longmaxi shale in the sichuan basin and adjacent areas. *Int. J. Coal Geol.* **2024**, *295*, 104642. [CrossRef]
58. Wang, M.; Su, X.; Song, H.; Wang, Y.; Yang, X. Enhancing predictive maintenance strategies for oil and gas equipment through ensemble learning modeling. *J. Pet. Explor. Prod. Technol.* **2025**, *15*, 46. [CrossRef]
59. Yang, Y.; Zhang, X.; Zhou, X.; Wang, A.; Li, J. Experimental analysis of the pore structure, relative permeability, and water flooding characteristics of the Yan'an Formation sandstone, southwestern Ordos Basin. *Energy Geosci.* **2023**, *4*, 100184. [CrossRef]
60. Homke, S.; Vergés, J.; Van Der Beek, P.; Fernàndez, M.; Saura, E.; Barbero, L.; Badics, B.; Labrin, E. Insights in the exhumation history of the nw zagros from bedrock and detrital apatite fission-track analysis: Evidence for a long-lived orogeny. *Basin Res.* **2010**, *22*, 659–680. [CrossRef]
61. Wu, R.; Zhang, C.; Wang, R.; Sun, Q.; Song, G.; Shi, M. A novel numerical simulation study on the flow mechanisms of deep low-permeability gas reservoirs. *J. Pet. Explor. Prod. Technol.* **2025**, *15*, 43. [CrossRef]
62. Zeng, S.; Zhang, J.; Zhang, H.; Li, R.; Ao, T.; Cao, K. Experimental study on erosion modeling of architectural red sandstone under the action of the natural environment. *Buildings* **2024**, *14*, 1168. [CrossRef]
63. Liu, C.; Sun, L.; Lu, J.; Sun, Y.; Xu, Y.; Lu, M.; Li, J. Characteristics of the newly found oil-bearing sandstone in the denglouku formation of the northern songliao basin, China. *J. Pet. Sci. Eng.* **2020**, *188*, 106947. [CrossRef]
64. Zou, J.; Wang, W.; Liu, C. Types of sedimentary facies of palace area in songliao basin. In Proceedings of the International Symposium on Computers and Informatics (ISCI), Beijing, China, 17–18 January 2015; pp. 2361–2368.
65. Liu, Y.C.; Xu, D.L.; Liu, C.Z.; Li, L.Q.; Pei, J.B. Diagenesis of volcanic rocks and its effects on evolution of reservoir space of yingcheng formation in 2,3 wellblock of yaoshen area. In Proceedings of the 3rd International Conference on Advanced Design and Manufacturing Engineering (ADME 2013), Anshan, China, 13–14 July 2013; pp. 455–458. [CrossRef]

Disclaimer/Publisher's Note: The statements, opinions and data contained in all publications are solely those of the individual author(s) and contributor(s) and not of MDPI and/or the editor(s). MDPI and/or the editor(s) disclaim responsibility for any injury to people or property resulting from any ideas, methods, instructions or products referred to in the content.